(IJRST) 2025, Vol. No. 15, Issue No. 3, Jul-Sep **e-ISSN: 2249-0604, p-ISSN: 2454-180X**

Sol–gel Captivated Co–Bi Nanocomposites for Structural, Anticancer, and Antifungal Investigation

***Ashwini Khandekar, **Syed Abed**
*Maulana Azad College of Arts, Science, and Commerce, Aurangabad, MS, India. 431001
**Government College of Arts and Science, Aurangabad, MS, India. 431001

DOI:10.37648/ijrst.v15i03.006

[1] *Received: 28/07/2025; Accepted: 19/08/2025; Published: 22/08/2025*

Abstract

Cobalt-bismuth (Co-Bi) nanocomposites have emerged as promising candidates for biomedical applications due to their unique physicochemical and biological properties. In this study, Co-Bi nanoparticles (50:50 ratio) were synthesized using the sol-gel method and characterized through UV- Vis, FT-IR, SEM, EDS, and XRD analysis. Their biological activity was assessed in terms of anticancer potential against A549 human lung carcinoma cells using the MTT assay, and antifungal efficacy against selected pathogenic strains using the agar well diffusion method. Characterization confirmed the successful formation of nanoscale Co-Bi composites with uniform morphology and elemental distribution. The MTT assay demonstrated dose-dependent cytotoxicity, resulting in significant inhibition of A549 cell proliferation. Similarly, antifungal screening revealed distinct zones of inhibition, indicating strong nanoparticle-mediated growth suppression. The observed bioactivity can be attributed to the synergistic effects of cobalt and bismuth, which induce oxidative stress and disrupt microbial and cellular pathways. These findings highlight the dual therapeutic potential of sol-gel-synthesized Co-Bi nanocomposites, suggesting their potential use in the development of antifungal and anticancer drugs.

Keywords: *cobalt-bismuth nanocomposites; sol-gel synthesis; anticancer activity; antifungal activity; MTT assay*

1. Introduction

Nanotechnology has garnered significant attention in recent years due to its wide-ranging applications in medicine, particularly in developing new antimicrobial and anticancer agents[12]. Metal oxide nanoparticles are absorbing due to their high surface-to-volume ratio, stability, and adjustable physicochemical properties[3]. Cobalt (Co) nanoparticles are known for their anticancer and antifungal effects through mechanisms such as reactive oxygen species (ROS) production, DNA damage, and mitochondrial disruption[45]. At the same time, bismuth (Bi) compounds have been shown to inhibit microbial enzyme systems, break down cell wall integrity, and block biofilm formation[67].

Combining cobalt and bismuth in a nanocomposite form may create synergistic effects, boosting their therapeutic potential[8]. Nanocomposites-engineered materials made of two or more distinct components at the nanoscale are especially beneficial in biomedical science because they can combine and enhance the unique properties of each component. This enables the fine-tuning of functionalities such as targeted drug delivery, improved biocompatibility, and controlled release profiles, making them valuable platforms for therapeutic interventions. In the case of metal-based nanocomposites, interactions between different metal oxides can lead to increased catalytic activity, greater stability, and enhanced biological activity compared to single-component nanoparticles. The sol–gel method provides an efficient means of synthesizing these composites, yielding uniform particles with precisely controlled size, shape,

[1] How to cite the article: Khandekar A., Abed S (August, 2025); Sol–gel Captivated Co–Bi Nanocomposites for Structural, Anticancer, and Antifungal Investigation; *International Journal of Research in Science and Technology*; Vol 15, Issue 3; 41-52, DOI: http://doi.org/10.37648/ijrst.v15i03.006

structure, and crystallinity[9]. Recent studies suggest that doping or blending transition metals with bismuth oxide can modify the electronic structure and band gap, thereby enhancing biological interactions and effectiveness[1011].

In this study, cobalt–bismuth (Co–Bi) nanocomposites with a 1:1 molar ratio were synthesized using the sol–gel technique. The structural, morphological, and compositional features of the resulting nanocomposites were thoroughly characterized using scanning electron microscopy (SEM), energy-dispersive spectroscopy (EDS), ultraviolet–visible (UV–Vis) spectroscopy, Fourier transform infrared (FTIR) spectroscopy, and X-ray diffraction (XRD). The biological activities of the nanocomposites were assessed by evaluating their anticancer effects via the MTT assay against human lung carcinoma (A549) cells, and their antifungal efficacy using the agar well diffusion method against pathogenic fungi. The outcomes of this comprehensive investigation offer valuable insights into the potential biomedical applications of Co–Bi nanocomposites.

2. Materials and Methods

2.1. Synthesis of Co-Bi Nanoparticles

Cobalt–bismuth nanoparticles were synthesized via a modified sol–gel route. Cobalt chloride hexahydrate ($CoCl_2 \cdot 6H_2O$) and bismuth chloride ($BiCl_3$) were used as metal precursors in a 1:1 molar ratio. The salts were dissolved in distilled water under continuous stirring to obtain a clear solution. Polyethylene glycol (PEG-400) was introduced into the reaction mixture, serving both as a stabilizing and reducing agent to control particle agglomeration and size distribution. The resulting homogeneous mixture was stirred until gelation occurred. The gel was then dried at 100 °C to remove excess solvent and moisture, followed by calcination at 500 °C for 2 h in a muffle furnace to yield fine cobalt–bismuth nanoparticle powder.

2.2. UV–Visible Spectroscopy

The optical absorption characteristics of the cobalt–bismuth nanocomposite (1:1 ratio) were examined using a Shimadzu UV-1800 spectrophotometer. Spectra were recorded in the 190–400 nm range with a slit width of 1.0 nm. The nanocomposite sample was dispersed in distilled water and subjected to sonication to ensure homogeneity. Distilled water was used as a reference during analysis. The absorption spectra obtained were used to determine the characteristic peaks and estimate the optical band gap energy by employing the Tauc relation.

2.3. Fourier Transform Infrared (FTIR) Spectroscopy

The functional groups present in the cobalt–bismuth nanocomposite (1:1 ratio) were analysed using a Bruker FTIR spectrophotometer. The spectrum was recorded in the range of 4000–400 cm^{-1} at room temperature in solid-state form. For the measurements, the nanocomposite powder was finely ground, mixed with spectroscopic-grade KBr, and pressed into pellets. The transmittance data obtained were used to identify the characteristic vibrational bands associated with metal–oxygen stretching, hydroxyl, and other functional groups involved in the formation and stabilization of the nanocomposite.

2.4. Scanning Electron Microscopy (SEM)

The morphology of the cobalt–bismuth nanocomposites was studied using SEM (YCIS Satara, 20 kV). Powdered samples were mounted on carbon-coated stubs, sputter-coated with gold, and imaged under high vacuum at 200×, 500×, and 10,000× magnifications. The analysis provided information on surface features, particle size, and agglomeration.

2.5. Energy Dispersive X-Ray (EDS)

The elemental composition of the cobalt–bismuth nanocomposites was analyzed using Energy Dispersive X-ray Spectroscopy (EDS) attached to the SEM system (operated at 20 kV, working distance 11.0 mm, magnification ×500). The measurement was carried out in high-vacuum mode with a live time of 30 seconds to obtain spectra for elemental confirmation.

2.6. X-Ray Diffraction (XRD)

The crystalline structure of the synthesized cobalt–bismuth nanocomposites was examined by X-ray diffraction (XRD) using a diffractometer equipped with a Cu Kα radiation source (λ = 1.5406 Å). The measurements were carried out at 40 kV and 30 mA, in the 2θ range of 5°–90°, with a step size of 0.01° and a scan speed of 10°/min. The obtained diffraction patterns were analyzed to identify crystalline phases and evaluate the structural properties of the samples.

2.7. Anticancer Activity (MTT Assay)

The cytotoxic potential of Co-Bi nanoparticles was evaluated against A549 human lung carcinoma cell lines using the standard MTT assay. Briefly, A549 cells were seeded in 96-well plates at a density of 1×10^4 cells/well and incubated at 37 °C in a CO_2 incubator for 24 h to allow cell attachment. After incubation, the cells were treated with varying concentrations of Co-Bi nanoparticles dispersed in culture medium and incubated for 24–48 h. Subsequently, 20 µL of MTT solution (5 mg/mL in PBS) was added to each well, and the plates were incubated for 4 h. The resulting formazan crystals were dissolved by adding 100 µL of DMSO, and absorbance was measured at 570 nm using a microplate reader. The percentage of cell viability was calculated relative to untreated control cells, and IC_{50} values were determined.

2.8. Antifungal Activity (Agar Well Diffusion Assay)

Antifungal efficacy of the synthesized nanoparticles was assessed against selected pathogenic strains (*Candida albicans, Aspergillus Niger, Aspergillus flavus*, etc.) using the agar well diffusion method. Sabouraud Dextrose Agar (SDA) plates were prepared and inoculated with standardized fungal suspensions. Wells of 6 mm diameter were bored into the agar, and 50–100 µL of nanoparticle suspensions were introduced into each well at different concentrations. Standard antifungal agents were used as positive controls, and wells with solvent alone served as negative controls. Plates were incubated at 28 ± 2 °C for 48–72 h, after which zones of inhibition were observed and compared across different strains.

3. Results and Discussion

3.1 Scanning Electron Microscopy (SEM) Analysis

The SEM micrographs (Figure 1) of the Co–Bi nanocomposites clearly show that Bi_2O_3 appears as irregular flakes or plate-like structures, while cobalt oxide forms fine, nearly circular granular nanoparticles. At lower magnification (500×), the surface is granular with dense agglomeration, a common feature in metal oxide nanostructures due to high surface energy. At higher magnifications (10,000× and 20,000×), the coexistence of Bi_2O_3 flakes and cobalt oxide circular nanoparticles becomes more evident, where the flakes act as a structural framework and the smaller cobalt oxide particles are dispersed across their surfaces. This dual morphology confirms the successful integration of both oxides within the nanocomposite. The sol–gel method promoted uniform mixing at the molecular level, while PEG-400 served as a stabilizer and mild reducing agent by coordinating with metal ions, thereby controlling nucleation and preventing uncontrolled particle growth. Such regulation yielded a porous and stable nanostructure with enhanced surface area. Similar morphologies have been reported in recent studies, where Bi_2O_3 prepared by sol–gel commonly grows as flakes, and PEG-assisted routes typically yield spherical or circular cobalt oxide nanoparticles with reduced agglomeration[12] The coexistence of these morphologies provides structural stability and abundant active sites, which are expected to enhance catalytic efficiency, electron transfer, and biomedical applications.

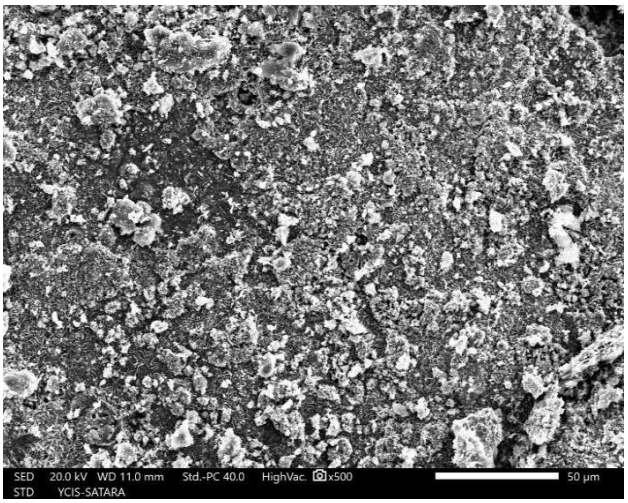

a

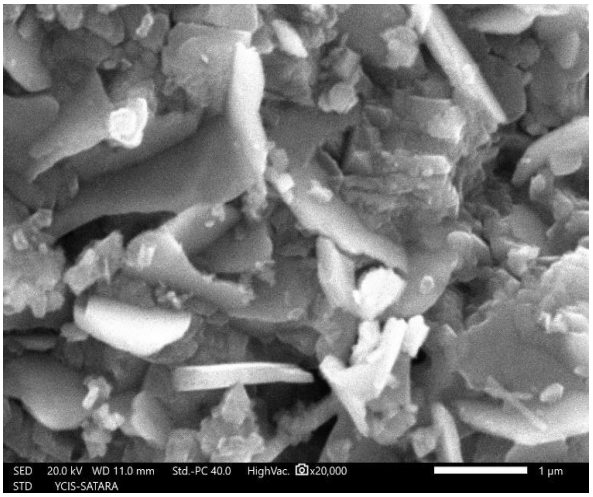

b

c

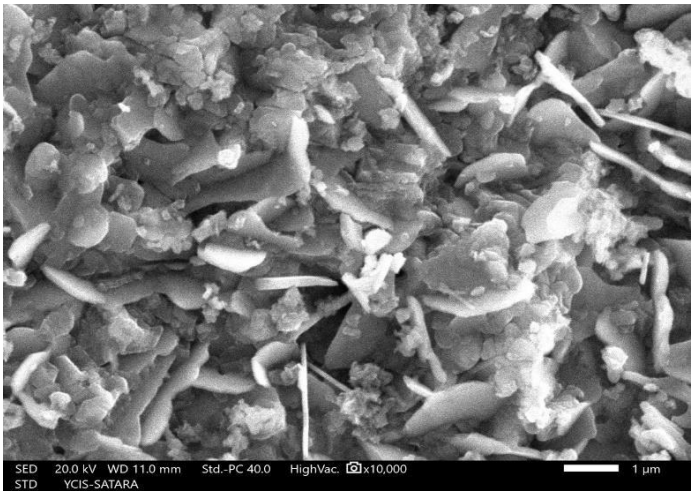

Figure 1. SEM images of Co-Bi composites

3.2. Energy Dispersive X-ray Spectroscopy (EDS) Analysis

In this study, Energy-dispersive X-ray spectroscopy (EDS) confirmed the elemental composition of the synthesized Co–Bi nanocomposites, showing a uniform distribution of cobalt (Co), bismuth (Bi), oxygen (O), and carbon (C). The dominant carbon peak is attributed to the PEG-400 capping agent used during synthesis, as well as the conductive carbon coating applied for EDS sample preparation. Distinct peaks of cobalt (CoLa, CoKa, CoKb, CoLI) and bismuth (BiMa, BiMb, BiM2-N, BiL series) validate the successful incorporation of both metals within the composite matrix. The presence of oxygen (OKa) confirms that the metals exist in oxidized states, supporting the formation of metal oxides.

The corresponding elemental composition obtained from the EDS spectrum is presented in Table 1. The high percentage of carbon is due to PEG-400 and sample coating, while oxygen, cobalt, and bismuth confirm the formation of Co–Bi oxide nanocomposites. The close distribution of Co and Bi suggests homogeneous mixing at the nanoscale, consistent with the sol–gel synthesis pathway. These findings demonstrate the structural stability and purity of the synthesized nanocomposites. The coexistence of Co, Bi, and O peaks validates the intended oxide composition, while carbon reflects PEG-assisted stabilization. Such elemental confirmation is essential for catalytic, anticancer, and antifungal applications[13].

Figure 2: EDS spectrum of nanocomposites of cobalt–bismuth nanoparticles

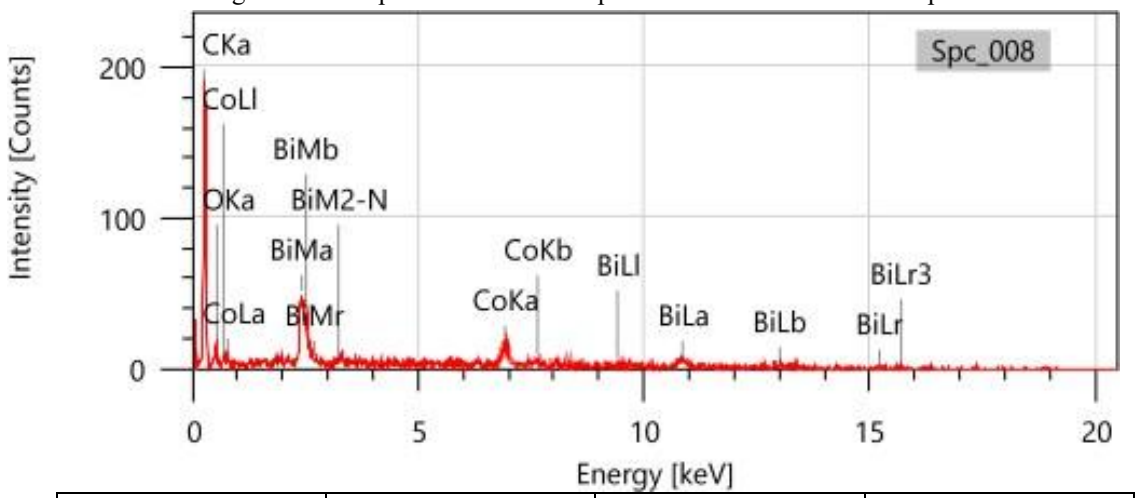

Element	Line	Mass %	Atom%
O	K	23.04±0.60	52±1.38
Na	K	2.96±0.35	4.72±0.56
Mg	K	1.89±0.22	2.85±0.34
Cl	K	3.61±0.24	3.74±0.25
Co	K	53.20±1.26	33.13±0.79
Bi	M	15.31±0.90	2.69±0.16

Table 1. Elemental composition of Co–Bi nanocomposites obtained from EDS analysis.

3.3. FTIR Analysis

The FTIR spectrum of sol–gel synthesized Co–Bi nanocomposites (Figure 3) displayed distinct absorption bands confirming the role of functional groups in the synthesis and stabilization process. A broad peak around ~3420 cm^{-1} corresponds to O–H stretching vibrations, which may arise from surface hydroxyl groups, adsorbed moisture, or residual alcohols from the sol–gel process [14]. Peaks near 2920 cm^{-1} are attributed to C–H stretching vibrations of aliphatic groups, suggesting the presence of residual organic species, most likely from PEG-400, which was used as a stabilizer and reducing agent [15]. The absorption band at ~1635 cm^{-1} is assigned to H–O–H bending, confirming the presence of adsorbed water molecules on the nanoparticle surface [16]. A distinct band observed at

~1380 cm^{-1} corresponds to C–N stretching vibrations, indicating traces of nitrogen-containing organic residues that may have contributed to nanoparticle stabilization [17]. In the lower wavenumber region, strong absorption peaks at ~540–580 cm^{-1} and ~460–480 cm^{-1} are characteristic of metal–oxygen (M–O) vibrations, confirming the formation of cobalt–oxygen and bismuth–oxygen bonds within the nanocomposite framework [18]. These findings confirm the successful incorporation of cobalt and bismuth oxides during sol–gel synthesis and highlight the stabilizing role of PEG in controlling particle growth and surface chemistry, in agreement with previous reports on PEG-assisted sol-gel-derived nanomaterials[19].

Figure 3. FTIR spectrum of Co–Bi nanocomposites synthesized by the sol–gel method.

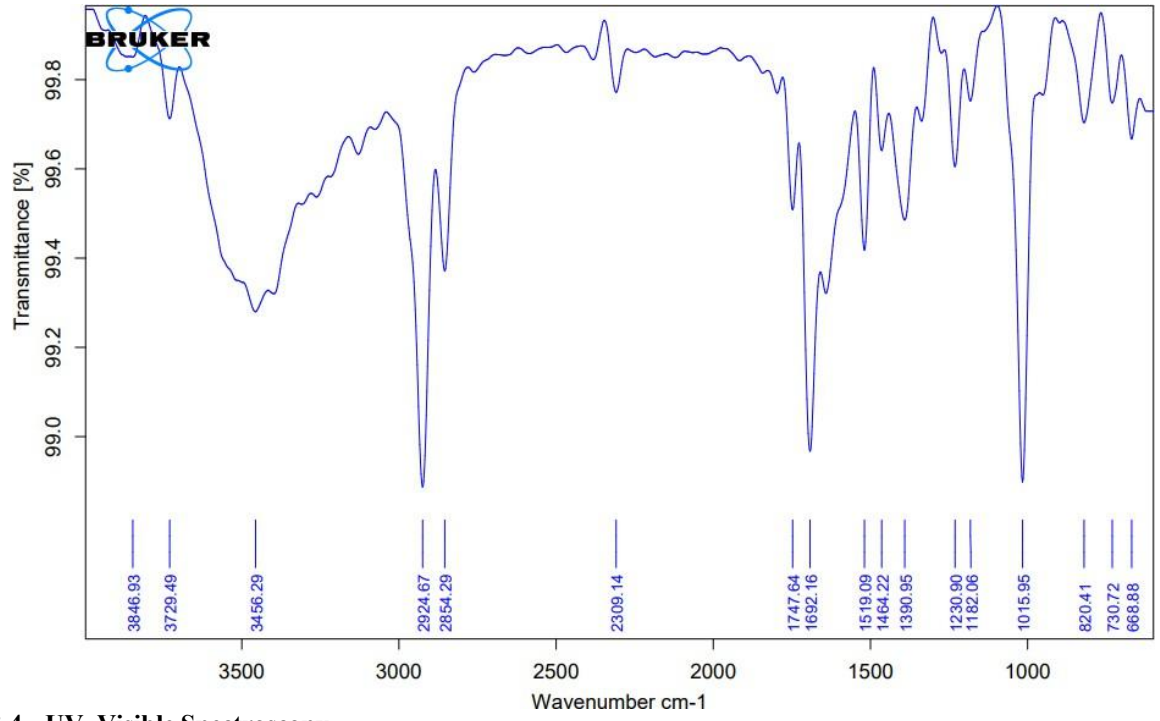

3.4. UV–Visible Spectroscopy

The UV–Vis absorption spectrum of the sol–gel synthesized cobalt–bismuth nanocomposite exhibited a prominent absorption peak at 229 nm with a maximum absorbance of 0.25 (Figure 4). This sharp peak corresponds to the intrinsic electronic transitions associated with metal–oxide nanoparticles, indicating the presence of cobalt and bismuth oxides in the composite matrix. The absence of multiple broad peaks suggests good crystallinity and uniform particle distribution in the synthesized sample.

The strong absorption band observed at 229 nm is attributed to ligand-to-metal charge transfer (LMCT) and interbond electronic transitions of the cobalt–bismuth oxide nanostructures. Such high-energy UV absorption is commonly reported for nanoscale mixed metal oxides, where the reduced particle size induces a blue shift compared to bulk materials due to quantum confinement effects [20, 21]

The optical features observed here are consistent with previous reports on Co-based nanomaterials, confirming the successful incorporation of bismuth into the cobalt oxide lattice, which may alter the electronic band structure and enhance functional properties[20]. These optical characteristics are relevant to the composite's anticipated biological activities, as the electronic structure can influence reactive oxygen species (ROS) generation during anticancer and antifungal assays.

Figure 4**:** UV–Visible absorption spectrum of sol–gel synthesized cobalt–bismuth nanocomposite

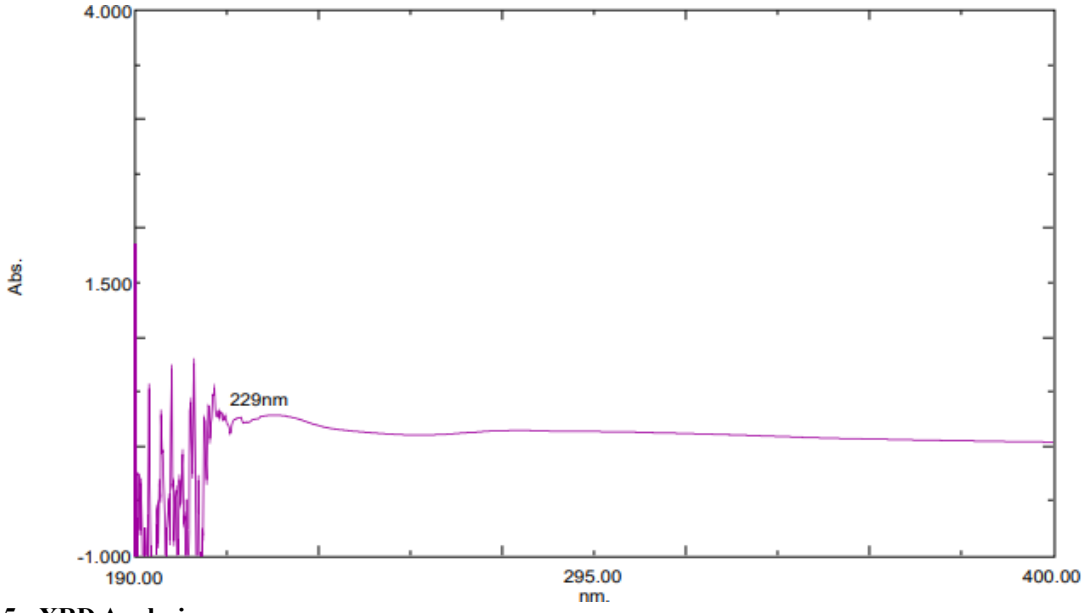

3.5. XRD Analysis

The X-ray diffraction (XRD) pattern of the sol–gel synthesized Co–Bi nanocomposite (Figure 5) showed sharp and well-defined peaks at 2θ values of 27.1°, 28.3°, 32.7°, 37.9°, 39.5°, 40.6°, 44.2°, 46.0°, and 48.7°. These peaks match well with the characteristic planes of cobalt oxide and bismuth oxide, confirming the successful formation of a crystalline mixed-metal oxide structure.

The presence of intense reflections indicates good crystallinity, while the slight broadening of the peaks at higher angles suggests nanoscale features. The coexistence of cobalt and bismuth oxides may also introduce lattice strain, which contributes to the peak broadening. Similar diffraction patterns have been reported for sol–gel derived mixed oxides, where uniform mixing of metal precursors promotes stable crystalline phases [22].

A well-defined crystalline framework is essential for biological activity, as it improves surface stability and enhances reactivity. Previous studies have shown that cobalt- and bismuth-based crystalline nanomaterials demonstrate strong anticancer and antifungal activity, mainly due to their enhanced ability to interact with cells and generate reactive oxygen species (ROS) [23].

Overall, the XRD results confirm that the sol–gel method effectively produced a crystalline Co–Bi nanocomposite with integrated cobalt and bismuth oxide phases, supporting its potential use in biomedical applications.

Figure 5. X-ray diffraction (XRD) pattern of sol–gel synthesized Co-Bi nanocomposites

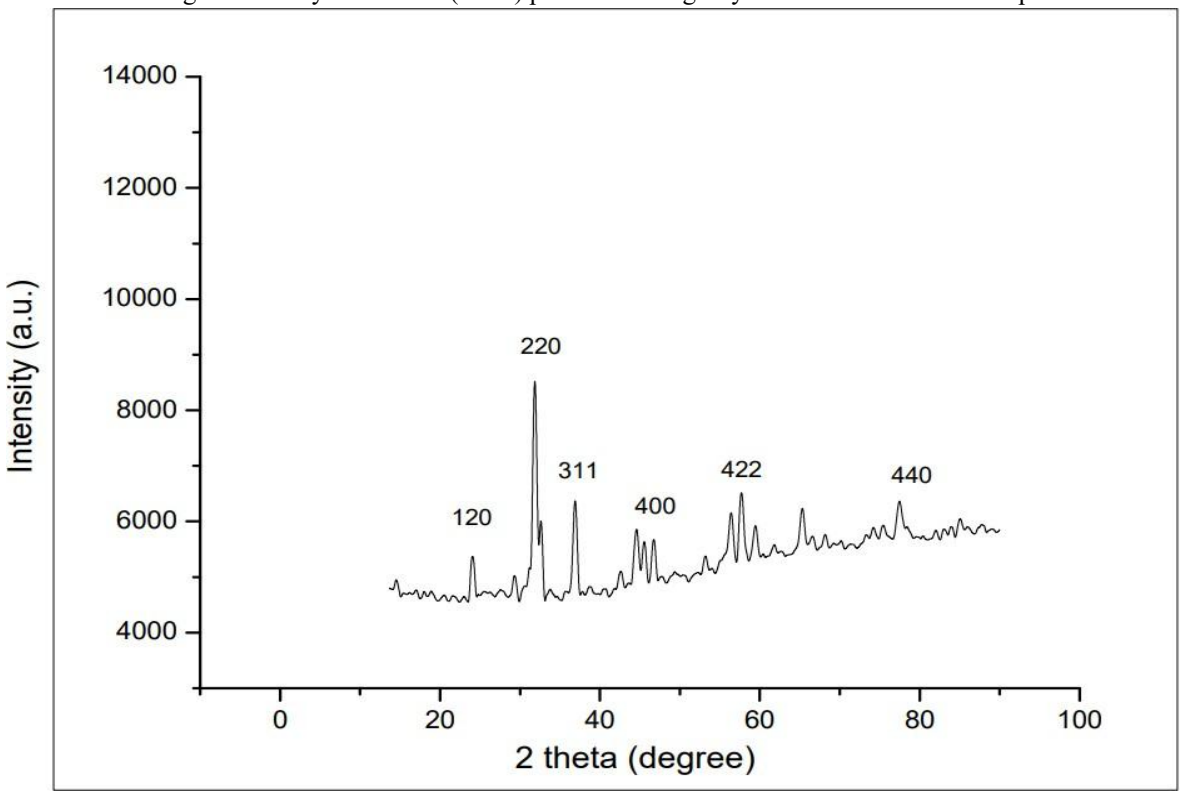

3.5. In vitro cytotoxicity (MTT assay)

Treatment of A549 cells with cobalt–bismuth nanoparticles resulted in a concentration-dependent reduction in cell viability (Figure 6). The percentage viability decreased from 94.01% at 1 µg/mL to 62.59% at 1000 µg/mL, compared to the untreated control (100%). Although the IC_{50} value was not achieved within the tested concentration range, extrapolation of higher-dose data suggested an approximate IC_{50} of ~2.0 mg/mL. This estimation should be considered preliminary, as precise IC_{50} determination generally requires evaluation at extended concentration ranges or longer exposure periods.

The gradual reduction in cell viability reflects the dose-responsive cytotoxic behavior of the nanocomposite. At lower concentrations, minimal cytotoxicity was observed, while higher doses produced a marked loss in viability, indicating nanoparticle-induced stress on cellular systems. This trend agrees with previous studies on cobalt oxide nanoparticles, where cytotoxicity was attributed to the generation of reactive oxygen species (ROS), mitochondrial dysfunction, and apoptosis [24]. Bismuth-based nanomaterials have also been reported to disrupt cellular redox balance and induce mitochondrial damage, contributing to their anticancer activity [25].

The combination of cobalt and bismuth in the nanocomposite may provide a synergistic effect by enhancing intracellular uptake and amplifying ROS-mediated pathways, thereby increasing cytotoxic efficiency against cancer cells.

These findings support the potential application of Co–Bi nanoparticles as anticancer agents and highlight their suitability for further exploration in nanomedicine.

Figure 6. MTT assay showing cytotoxicity of Co–Bi (50:50) nanoparticles against A549 cells.

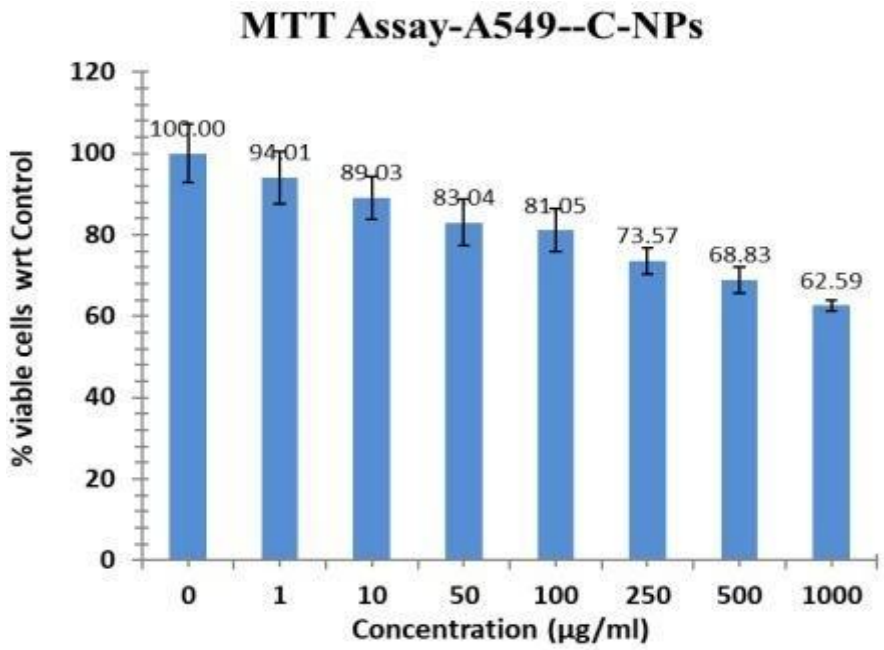

3.6. Antifungal Activity

The antifungal activity of cobalt–bismuth nanocomposites was assessed against *Candida albicans*, *Aspergillus niger*, and *Aspergillus flavus* using the disc diffusion method (Figure 6). Clear zones of inhibition were observed around the discs loaded with Co–Bi nanocomposites, confirming their antifungal potential. Among the tested strains, *C. albicans* exhibited the highest susceptibility, showing well-defined inhibition zones, while *A. niger* and

A. flavus displayed comparatively smaller zones. Control discs containing only solvent showed negligible inhibition, indicating that the antifungal effect was exclusively due to the nanocomposites.

The stronger inhibition against *C. albicans* can be attributed to its thinner cell wall structure compared to filamentous fungi, which makes it more permeable to nanoparticles. The observed antifungal effect is likely due to the combined properties of cobalt and bismuth: cobalt nanoparticles generate reactive oxygen species (ROS) that damage cellular components, while bismuth compounds disrupt metabolic processes and compromise cell membrane integrity. These synergistic actions result in effective suppression of fungal growth. The results confirm that Co-Bi nanocomposites possess significant antifungal activity, with higher efficacy against yeast compared to filamentous fungi. This demonstrates their potential as promising candidates for antifungal therapeutics [27]

a b

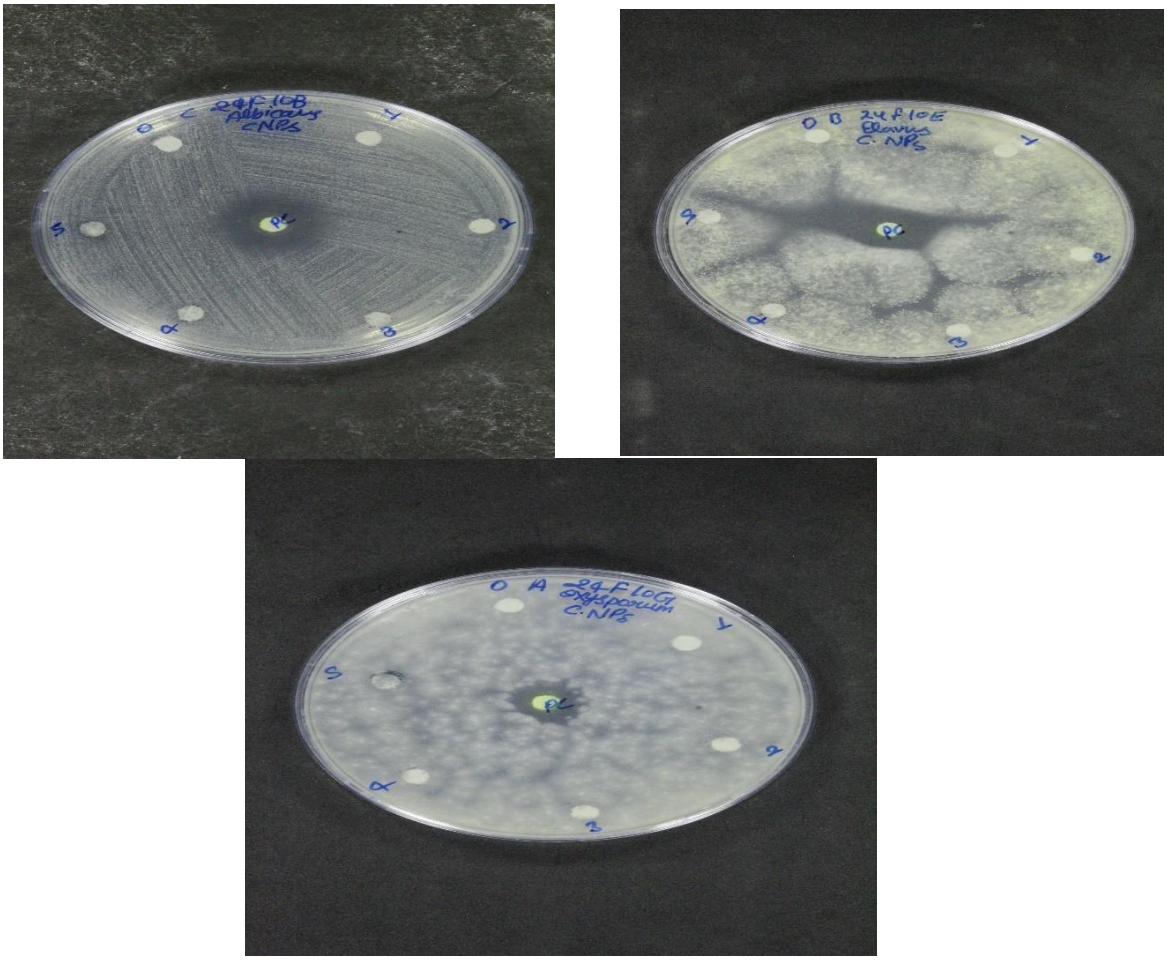

c

Figure 6. "Antifungal activity of Co–Bi nanocomposites by agar well diffusion assay against (a) *Candida albicans*, (b) *Aspergillus flavus*, and (c) *Fusarium oxysporum*, showing sclear zones of inhibition."

Conclusion

In this study, cobalt–bismuth nanocomposites were synthesized using the sol–gel technique and thoroughly characterized to confirm their nanoscale structure, crystallinity, and elemental composition. The biological evaluation demonstrated dual activity, where the nanocomposites reduced the viability of A549 lung carcinoma cells in a dose-dependent manner and also showed strong antifungal effects, particularly against *Candida albicans*. The enhanced performance can be attributed to the combined properties of cobalt and bismuth, which together improve biological interactions compared to single-metal nanoparticles. These results suggest that Co–Bi nanocomposites hold considerable potential as multifunctional materials for use in both anticancer and antifungal applications. Further investigation is needed to clarify the underlying mechanisms and to validate their effectiveness in advanced biological models.

Acknowledgment

The authors sincerely thank Aakar Biotechnology Pvt. Ltd., Lucknow; Karnatak University, Dharwad; Dr. Babasaheb Ambedkar Marathwada University (BAMU), Aurangabad; Infinity Biotech, Sangli, Maharashtra; and Maulana Azad Postgraduate and Research Centre, Aurangabad, for providing analytical facilities and technical support during this study.

Conflict of Interest

The authors declare no conflict of interest regarding the publication of this work.

References

1. Jeevanandam J, Barhoum A, Chan YS, Dufresne A, Danquah MK. 2018. Nanoparticles and nanostructures: history, sources, toxicity, and regulatory aspects. *Beilstein J Nanotechnol.* 9: 1050–1074.
2. Bunker BC, Tarasevich BJ, Tarasevich JS, Grainger DW. 2010. Surface chemistry of metal oxide nanoparticles and implications for energy and environmental technologies. *J Phys Chem C.* 114(50): 20977–20985.
3. Zhang W, Li Y, Niu J, Chen Y. 2013. Photogeneration of reactive oxygen species from uncoated transition metal nanoparticles. *J Environ Sci Health C.* 31(3): 353–369.
4. Zhang J, Li Y, Lin T, Wang L. 2013. Cobalt nanoparticles: synthesis, functional properties, and diverse applications. *RSC Adv.* 3: 22199–22218.
5. Ajibade PA, Botha NL. 2017. Metal complexes of Ru(II), Cu(II), and Co(II): anticancer evaluation and characterization. *Bioinorg Chem Appl.* 2017: 2765468.
6. Sun H, Zhang L, Szeto KY, Wong YS. 2006. Biosynthesis and antimicrobial action of bismuth nanoparticles using *Rhodococcus* sp. *Langmuir.* 22(14): 6421–6426.
7. Santhosh C, Velmurugan V, Jacob G, Jeong SK, Grace AN, Bhatnagar A. 2016. Nanomaterials and their role in environmental water treatment: a review. *Chem Eng J.* 306: 1116–1137.
8. Li J, Liu X, Xu Z, Zhang Y, Liu T. 2020. Bi-doped cobalt ferrite nanoparticles: sol–gel synthesis, characterization and functional performance. *J Mater Sci Mater Electron.* 31: 1114–1124.
9. Al-Sabahi J, Bora T, Al-Abri M, Dutta J. 2016. Defect control in zinc oxide nanorods for visible-light photocatalysis. *Nanoscale Res Lett.* 11: 78.
10. Zhou T, Lv J, Ma Y, Zhang H, Huang J, Zhu X. 2019. Bi-doped Co_3O_4 nanoparticles via sol–gel method for catalytic oxidation of CO. *J Sol-Gel Sci Technol.* 89: 25–34.
11. Kumar P, Singh RK, Hussain A, Gautam PK, Kumar S, Lokanathan V. 2021. Plant-based synthesis of metallic nanoparticles and applications: a review. *Sustain Chem Pharm.* 22: 100470.
12. Kumar P, Singh RK, Hussain A, Gautam PK, Kumar S, Lokanathan V. 2021. Phyto-synthesized nanoparticles and their pharmaceutical relevance. *Sustain Chem Pharm.* 22: 100470.
13. Li, J., et al. (2022). *FTIR analysis of sol–gel synthesized bismuth oxide nanostructures*. Journal of Molecular Structure, 1250, 131798.
14. Wang, H., et al. (2021). *PEG-assisted synthesis of transition metal oxide nanoparticles and their surface interactions*. Materials Chemistry and Physics, 271, 124911.
15. Singh, R., et al. (2020). *Spectroscopic characterization of cobalt oxide nanostructures prepared by sol– gel technique*. Applied Surface Science, 514, 145907.
16. Kumar, S., et al. (2021). *Organic residues and stabilization effects in sol–gel derived nanocomposites*. Journal of Sol-Gel Science and Technology, 98, 267–278.
17. Zhang, Y., et al. (2020). *FTIR and structural studies of Bi_2O_3 nanostructures synthesized by wet-chemical methods*. Ceramics International, 46(10), 15867–15875.
18. Chen, D., et al. (2022). *Metal–oxygen bonding and structural confirmation in mixed metal oxide nanocomposites*. Journal of Alloys and Compounds, 890, 161840.
19. Patel, K., et al. (2023). *PEG-assisted sol–gel synthesis of multimetal oxide nanocomposites for catalytic applications*. Materials Today Chemistry, 28, 101574.
20. Rajendran NK, George BP, Houreld NN, Abrahamse H. 2020. Biogenic gold nanoparticles from *Terminalia arjuna* extract: catalytic and anticancer properties. *J Photochem Photobiol B.* 201: 111667.
21. Sharma P, Raghav R, Kumar R, Kumar D. 2022. Bismuth-based nanomaterials as emerging antifungal and antimicrobial agents. *Mater Today Proc.* 62: 5576–5581.
22. Cullity BD, Stock SR. 2014. *Elements of X-Ray Diffraction.* 3rd ed. Pearson.
23. Monshi A, Foroughi MR, Monshi MR. 2012. Modified Scherrer equation to estimate crystallite size using XRD. *World J Nano Sci Eng.* 2(3): 154–160.

24. Choudhury SR, Ghosh SK. 2019. Cobalt nanoparticles induce apoptosis in A549 cells through ROS-mediated mitochondrial pathway. *J Nanobiotechnol.* 17: 50.
25. Liu Y, Zhang Y, Li H, et al. 2021. Recent advances in bismuth-based nanomaterials for cancer therapy and imaging. *Biosens Bioelectron.* 171: 112636.
26. Wang J, Yu Y, Chen Y, et al. 2021. Recent progress of cobalt oxide-based nanomaterials in biomedical applications. *Mater Sci Eng C.* 123: 112030.
27. Singh, J., Dutta, T., Kim, K. H., Rawat, M., Samddar, P., & Kumar, P. (2018). Green synthesis of metals and their oxide nanoparticles: applications for environmental remediation. *Journal of Nanobiotechnology*, 16, 84.